NUMERICAL STUDY OF THE PARAMETERS OF A LOW-DENSITY PLASMA THAT ABSORBS CO_2 LASER RADIATION

S. P. Popov and Yu. I. Romashkevich

UDC 533.6.011

Calculations have been made from the equations for nonstationary two-dimensional gasdynamics with allowance for the absorption of the laser radiation and for the possible deviations in the temperature and degree of ionization from the equilibrium values; the application is to heating and motion of a helium plasma produced by a 100-nsec CO_2 laser pulse of total energy 10 J. The mean charged-particle density is about 10^{18} cm^{-3}, while the maximum temperature is 25 eV and the size of the plasma formation is 0.2-1.2 cm.*

The breakdown in gases due to high-power laser pulses has long been a subject of research; theoretical descriptions of the breakdown are now in good qualitative agreement with the extensive experimental results, but quantitative agreement is obtained in much fewer cases. This is due to the existence of numerous physical processes. A more accurate allowance for charged-particle diffusion, electron energy loss in inelastic collisions, and the real laser intensity distribution requires the use of numerical methods.

A similar situation occurs in research on the interaction of laser radiation with the plasma produced by breakdown. Researchers in this area are concerned in particular with the scope for containing, compressing, and heating the not very dense plasma with magnetic fields, and also with self-focusing of the CO_2 laser beam in the plasma. Here we may mention [1-4] from the extensive literature on this topic. The most complicated feature in constructing a theoretical model is to calculate the gasdynamic motion, and this is possible only by numerical solution of the equations, after which one can draw conclusions on major characteristics such as the degree of ionization, the deviation from thermodynamic equilibrium, the spatial homogeneity, the speed of propagation of the boundaries, the absorption of the laser radiation, etc. The characteristic values of the electron temperature, charged-particle concentration, and spatial distribution allow one to examine the effects of reemission, electron thermal conduction, and so on which determine the transmission of the laser beam in the plasma. Such preliminary calculations allow one to identify the basic physical processes and therefore the set of equations to be solved.

There have been many constructions of algorithms for numerical simulation of the interaction of radiation with matter. The main attention has been given to the formation and heating of plasma in the exposure of solid targets to high-power monochromatic beams [5-7]. Of the recent studies concerned with laser breakdown in gases of normal density, we may note [8], where planar breakdown was examined on the basis of transport processes.

*Symbols: ρ, density; u, axial component of velocity; v, radial component of velocity; p, total pressure; E, total energy; ε, p_e, T_e, thermal energy, pressure, and temperature for electrons; T, temperature of atoms (ions); α_0, α_1, α_2, α_e, respectively, nonequilibrium atom concentration, concentrations of singly charged and doubly charged ions, and concentration of electrons; α_{0e}, α_{1e}, α_{2e}, α_{ee}, equilibrium values of these concentrations; K_1 and K_2, constants of ionization equilibrium; I_1 and I_2, ionization potentials of He; g_0, g_1, g_2, statistical weights; N_0, Loschmidt number; M, atomic mass; v_m, mean thermal velocity of electrons; σ_0, σ_1, σ_a, ionization cross sections of ions and atoms for electron impact and for atom–atom collision; σ_{0e}, σ_{1e}, σ_{2e}, cross sections for absorption of the laser radiation by electrons correspondingly in the fields of uncharged atoms and singly and doubly charged ions; $\varkappa_{0e}$, $\varkappa_{1e}$, $\varkappa_{2e}$, corresponding spectral linear absorption coefficients; $\varkappa$, linear absorption coefficient corrected for induced emission; t_a, t_i, t_{2i}, temperature-relaxation time corresponding to elastic collisions of electrons with atoms and ions; ν and q, quantum energy and flux density for radiation energy.

Translated from Zhurnal Prikladnoi Mekhaniki i Tekhnicheskoi Fiziki, No. 4, pp. 35-41, July-August, 1980. Original article submitted July 9, 1979.

0021-8944/80/2104-0462$07.50

Here we examine the motion of a low-density helium plasma heated by a CO_2 laser pulse. We consider only the two-dimensional character of the gasdynamic motion and the nonequilibrium processes of ionization and temperature establishment, while we examine the possible effects of electron thermal conduction and self-focusing from the final results. In this way one can determine the maximum gas density and radiation flux at which the flow model still applies.

The algorithm is based on splitting the system of equations. The gasdynamic part is solved by means of a two-dimensional Boris–Book scheme, while the equations for the kinetics of ionization and temperature relaxation are solved by the method of [9]. The experimental data of [10] were used for the characteristic dimensions of the irradiated gas volume, the initial temperature distribution, the charged-particle concentrations, and the length and power of the laser pulse. Only the geometry of the laser beam was altered: The conversion beam was replaced by two identical beams parallel to the axis of symmetry falling on the initially heated region from opposite sides. This simplifies the algorithm for calculating the course of the beam and gives us a symmetrical system, which increases the number of calculated points, which is very important in solving two-dimensional problems. The calculations of [11] have shown that one can neglect excitation of the atoms and radiation by the heated plasma in the working range of temperatures and densities. Under these circumstances the system of equations becomes

$$\begin{aligned}
&\frac{\partial \rho}{\partial t}+\frac{\partial \rho u}{\partial x}+\frac{\partial \rho v}{\partial r}+\frac{\rho v}{r}=0,\\
&\frac{\partial \rho u}{\partial t}+\frac{\partial\left(\rho u^2+p\right)}{\partial x}+\frac{\partial \rho u v}{\partial r}+\frac{\rho u v}{r}=0,\\
&\frac{\partial \rho v}{\partial t}+\frac{\partial\left(\rho v^2+p\right)}{\partial r}+\frac{\partial \rho v u}{\partial x}+\frac{\rho v^2}{r}=0,\\
&\frac{\partial E}{\partial t}\frac{\partial(E+p) u}{\partial x}+\frac{\partial(E+p) v}{\partial r}+\frac{(E+p) v}{r}=\varkappa q,\\
&\frac{\partial \rho \alpha_0}{\partial t}+\frac{\partial \rho \alpha_0 u}{\partial x}+\frac{\partial \rho \alpha_0 v}{\partial r}=f_0+f_1-\frac{\rho \alpha_0 v}{r},\\
&\frac{\partial \rho \alpha_2}{\partial t}+\frac{\partial \rho \alpha_2 u}{\partial x}+\frac{\partial \rho \alpha_2 v}{\partial r}+\frac{\rho \alpha_2 v}{r}=f_2,\\
&\frac{\partial \varepsilon}{\partial t}+\frac{\partial \varepsilon u}{\partial x}+\frac{\partial \varepsilon v}{\partial r}+p_e\left(\frac{\partial u}{\partial x}+\frac{\partial v}{\partial r}\right)+\frac{\left(\varepsilon+p_e\right) v}{r}=\varkappa q+\omega+\left(f_0+f_2\right) I_1-\left(I_1+I_2\right) f_2,\\
&\frac{\partial q}{\partial x}=-\varkappa q, \quad \alpha_0+\alpha_1+\alpha_2=1, \quad \alpha_e=\alpha_1+2\alpha_2.
\end{aligned} \tag{1}$$

The initial and boundary conditions of (1) will be described in detail in examining the results. Here and subsequently the following units are employed: T, T_e, I_1, I_2, ν, eV; $\rho_0 = MN_0 = 1.77\cdot10^{-4}$ g/cm³; $r_0 = 1$ cm; $u_0 = 0.5\cdot10^6$ cm/sec; $t_0 = 2\cdot10^{-6}$ sec. The system of (1) was supplemented with thermodynamic relations, which neglect the energy of electronic excitation in the atoms and ions:

$$\begin{aligned}
&\varepsilon = 3/2\rho T_e\alpha_e, \quad p_e = \rho T_e\alpha_e, \quad p = p_e + \rho T,\\
&E = \varepsilon + 3/2\rho T + \alpha_1\rho I_1 + \alpha_2\rho(I_1 + I_2) + \rho(u^2 + v^2)/2.
\end{aligned}$$

It was assumed that the nonequilibrium degrees of ionization α_1 and α_2 are defined by the reactions $A + e \rightleftarrows A^+ + 2e$, $A + A \rightarrow A^+ + e + A$, $A^+ + e \rightleftarrows A^{++} + 2e$; the second of these reactions was incorporated only for small degrees of ionization ($\alpha_e < 10^{-3}$). Then f_0, f_1, and f_2 appearing in (1) become

$$\begin{aligned}
&f_0 = -\alpha_0\alpha_e N_0\rho^2 t_0\sigma_0 v_m(I_1/T_e + 2)\exp(-I_1/T_e)\times(1 - \alpha_1\alpha_2/K_1\alpha_0),\\
&f_1 = \alpha_0\alpha_0 N_0\rho^2 t_0\sigma_a v_m(I_1/T + 2)\exp(-I_1/T),\\
&f_2 = \alpha_1\alpha_e N_0\rho^2 t_0\sigma_1 v_m(I_2/T_e + 2)\exp(-I_2/T_e)\times(1 - \alpha_2\alpha_e/K_2\alpha_1),\\
&K_{1.2} = \left(6.06\cdot10^{21} g_{1.2}/N_0\rho g_{0.1}\right) T_e^{3/2}\exp(-I_{1.2}/T_e),\\
&g_0 = g_2 = 1, \quad g_1 = 2, \quad v_m = 6.7\cdot10^7 T_e^{1/2},\\
&\sigma_0 = 0.13\cdot10^{-17} T_e, \quad \sigma_a = 10^{-19}, \quad \sigma_1 = 0.41\cdot10^{-18} T_e.
\end{aligned}$$

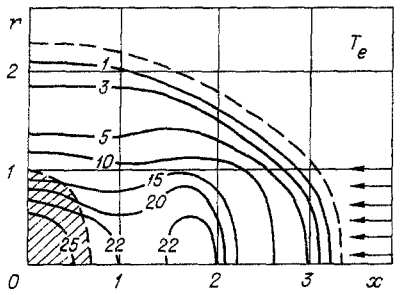

Fig. 1

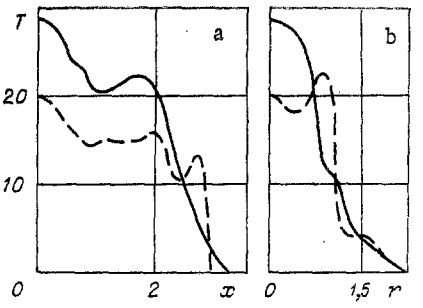

Fig. 2

The quantity ω, which governs the transmission of thermal energy from the electrons to the atoms and ions in elastic collisions, is put in the form $\omega = (1/t_a + 1/t_i + 1/t_{2i})(T - T_e)$; the cross sections appearing in t_a, t_i, t_{2i} were taken in accordance with [12]. The spectral linear absorption coefficient is

$$\varkappa = (\varkappa_{0e} + \varkappa_{1e} + \varkappa_{2e})(1 - \exp(-\nu/T_e)),$$
$$\varkappa_{0e} = \sigma_{0e}N_0^2\alpha_0\alpha_e\rho^2, \quad \varkappa_{1e} = \sigma_{1e}N_0^2\alpha_1\alpha_e\rho^2,$$
$$\varkappa_{2e} = \sigma_{2e}N_0^2\alpha_2\alpha_e\rho^2.$$

The cross section σ_{0e} was taken from [13], while σ_{1e} and σ_{2e} were taken in the hydrogen-like approximation of [12].

The following is the most characteristic of the series of calculations. At the initial instant, $\rho = 0.036$, $T_e = 0.025$ everywhere throughout the working region (which corresponds to a helium pressure of 30 mm Hg). Outside the region bounded by the ellipse $2x^2 + r^2 = 0.01$ (shown hatched in the diagrams), the state of the gas was considered to be that of thermodynamic equilibrium. Within the region $T_e = 2$, while α_1 and α_2 fall smoothly from the values $\alpha_1 = 0.1$ and $\alpha_2 = 0.05$ at the center to the values at the periphery. This distribution is close to predictions from breakdown theory. The radiation was assumed to propagate in a cylindrical channel of constant cross section and radius $r = 0.1$; one source acted on the region from the right (shown by arrows in Fig. 1), and the other from the left. The time course of the power in each pulse was $W = 10 \exp(-(30t - 0.75)^2)$. The pulse energy was 4.5 J and the radiation frequency in energy units was 0.116 eV. The calculations were performed over a uniform rectangular net. The step sizes in the difference net were the same in both spatial coordinates and were 0.15 mm.

The curves in Figs. 1a, b and 2a, b correspond to the instant of maximum laser power $t_1 = 51$ nsec. Figure 1 shows the lines of constant T_e, where the numbers on the curves are the values in eV, and x and r are everywhere in mm. The maximum plasma heating occurs in the region exposed to the laser radiation ($r < 1$ mm), and outside this region the temperature falls rapidly to 5-1 eV. There are two peaks in T_e; in the region of initial heating and at $x = 1.8$ mm. The position of the external shock wave is indicated by the broken line. The speed of this propagating against the laser beam is about 45 km/sec, while the lateral speed is 25 km/sec. Figure 2 shows the temperature nonuniformity in the plasma: curves *a* along the x axis for $r = 0$ and curves b along the r axis for $x = 0$. The broken line denotes the ion temperature T, while the solid line represents T_e. In the regions where $T_e > T$ (by about 30%) the disequilibrium is maintained in the main by the electron absorption, while in the region $T_e < T$ the difference is maintained mainly by the heating of the ion gas by the passage of the shock wave. This region is $2.2 < x < 2.8$ along the x axis. The external shock wave is weaker along the r axis, since it has emerged from the zone of the laser radiation, and T_e in it is close to T. However, at $r \gtrsim 1$ one finds the generation of a second shock wave, which raises the ion temperature. The formation of this is most readily detected from the behavior of the velocity.

To estimate the effects of electron thermal conduction we consider the spherically symmetrical problem of heat propagation with the initial distribution of T_e corresponding to the section $x = 1.8$ in Fig. 1, $N_e = 4 \cdot 10^{-2} N_0$; the equation of nonlinear thermal conduction was used with fitting. The calculations showed that T_e at the center fell from 22 to 16 eV in 10 nsec. On account of the nonlinearity ($\sim T_e^{2.5}$), the temperature distribution did not

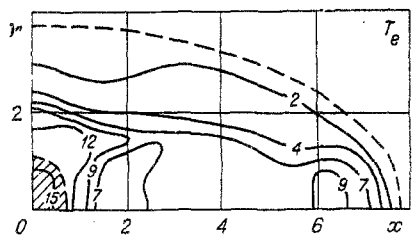

Fig. 3

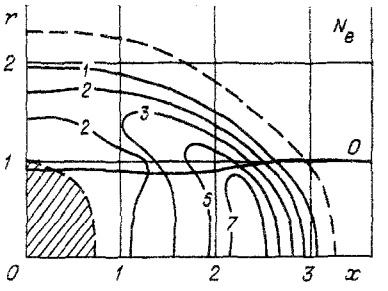

Fig. 4

vary appreciably in the region $T_e < 7$ eV. This indicates that the electron thermal conduction results essentially in equalization of the temperature profiles in the region $r < 1$ mm but has little effect on the process generally. As the laser pulse dies away, the temperature in the central region falls to 10-15 eV (Fig. 3 corresponds to $t_2 = 144$ nsec), and the electron thermal conduction plays no part. These calculations show that this case is a limiting one in the sense of the effects of the thermal conduction; T_e increases with the radiation flux and therefore the thermal conduction begins to play a considerable or even major part in the energy transport, while at lower fluxes the major mechanism is the hydrodynamic one (provided that the characteristic dimensions are retained). The speed of the external shock wave along the axis remains 45 km/sec, but along the r axis it falls roughly by a factor 1.5 by comparison with $t_1 = 51$ nsec and is 15 km/sec. With these initial conditions, there is up to 30% absorption of the laser radiation at the start of the process. Subsequently, the electron temperature rises and the density falls, and the proportion of energy absorbed in the perturbed region falls to a few percent.

Figures 4 and 5 show the electron density distribution for $t_1 = 51$ nsec, while Fig. 6 shows the same for $t_2 = 144$ nsec. The numbers on the lines give N_e in units of $2.687 \cdot 10^{17}$ $1/cm^3$. For example, number 2 corresponds to $N_e = 5.34 \cdot 10^{17}$ $1/cm^3$, etc. The minimum electron density occurs near the center and on the axis of symmetry in the ionized region; this provides [3, 4] self-focusing of a laser beam at an angle to the axis only on account of gasdynamic effects without influence from the external magnetic field. The distribution of N_e at t_1 was used in calculating the true optical path for the incident beam. This is denoted by 0 in Fig. 4. The propagation is initially parallel to the x axis, but then the region with increasing electron density acts as a positive lens, and the ray deviates from the axis by about 4-5° (the maximum linear deviation at $x = 1.8$ is 0.15 mm, which is the scale of one cell). The region $x < 1.5$ mm acts as a negative lens. As a result, the plasma has no substantial effect on the beam propagation. The same estimates were made for the N_e corresponding to 144 nsec, and the deviations from rectilinear propagation in that case were slight. This result is in agreement with experiment [10], where a self-focusing effect of 5-7° was observed. As the critical charged-particle concentration N^* is approached ($N^* = 0.9 \cdot 10^{19}$ $1/cm^3$ for $\nu = 0.116$ eV), the reflection and refraction increase considerably. In our example, the maximum value was $N_e = 0.2 \times 10^{19}$ $1/cm^3$, and therefore at pressures 3-4 times those used here (100-120 mm Hg) one would expect considerable effects from reflection and refraction of the beam.

Figure 5 compares α_e (solid lines) with the corresponding local-equilibrium values

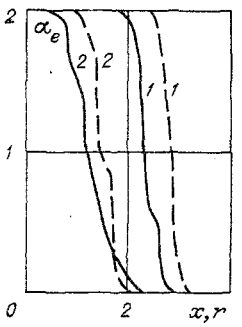

Fig. 5

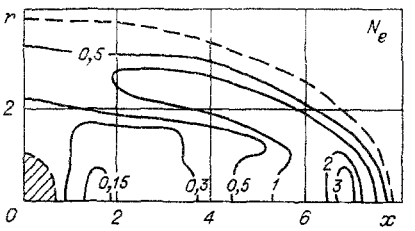

Fig. 6

(broken lines), where 1 denotes the distribution along the x axis and 2 the distribution along the r axis. The largest deviations occur in flow regions with $T_e < 2$-3 eV, where the ionization rate is less than or comparable with the rate of gasdynamic motion.

These calculations provide some general conclusions on the applicability of models; for example, they show that the motion of the plasma is essentially two-dimensional, which means that two-dimensional gasdynamic schemes must be used. There is also a substantial difference between the electron temperature and the ion temperature for virtually any parameters of the plasma at sufficiently high beam powers. Therefore, the two-temperature approximation should be used. Ionization nonequilibrium occurs only in regions with very low charged-particle concentrations or low electron temperatures (below 1-2 eV). These are peripheral regions of the plasma cloud in most problems of explosion type. It is difficult to foresee how far this disequilibrium will affect the flow as a whole in the calculations, so the equations for the ionization kinetics must be included. The effects of electron thermal conduction begin to make themselves felt at $T_e > 20$-30 eV, while nonlinearity in the beam propagation occurs for $N_e > (0.3\text{-}0.6)N^*$. The corresponding equations must then be used to supplement the ones used here. Emission from the plasma plays no part. Problems in laser interaction with plasma are very varied, and the above statements relate to a fairly narrow range in the plasma parameters and in the laser beam details.

We are indebted to O. S. Ryzhov and I. V. Nemchinov for their interest.

LITERATURE CITED

1. N. A. Amherd and G. G. Vlases, "Trapping and absorption of an axially directed CO_2 laser beam by a Θ-pinch plasma," Appl. Phys. Lett., 24, No. 2 (1974).
2. S. Y. Yuen, B. Lax, and D. R. Cohn, "Laser heating of a magnetically confined plasma," Phys. Fluids, 18, No. 7 (1975).
3. L. G. Johnson and T. K. Chu, "Measurements of electron density evolution and beam self-focusing in a laser-produced plasma," Phys. Rev. Lett., 32, No. 10 (1974).
4. D. R. Cohn, G. J. Raff, R. L. Brooks, N. G. Loter, and W. Halverson, "Beam self-focusing in a laser-produced plasma in a magnetic field," Phys. Lett., A49, No. 2 (1974).
5. Yu. V. Afanas'ev, N. G. Basov, et al., "Laser-induced fusion reaction in inhomogeneous spherical targets," Pisma Zh. Eksp. Teor. Fiz., 24, No. 1 (1976).
6. O. M. Belotserkovskii, V. V. Demchenko, V. I. Kosarev, and A. S. Kholodov, "Numerical simulation of some problems in laser compression of shells," Zh. Vychisl. Mat. Mat. Fiz., 18, No. 2 (1978).
7. A. A. Bunatyan, V. E. Neuvazhaev, L. P. Strotseva, and V. D. Frolov, Numerical Study of Perturbations in the Compression of a Target by a Sharpened Pulse [in Russian], Preprint IMP Akad. Nauk SSSR No. 71 (1975).
8. M. F. Ivanov, "Propagation of an optical breakdown wave in a gas," Kvantovaya Elektron., 5, No. 12 (1978).
9. S. P. Popov and Yu. I. Romashkevich, "A splitting method applied to calculations on two-temperature and nonequilibrium-ionized gas flows," Zh. Vychisl. Mat. Mat. Fiz., 17, No. 6 (1977).
10. T. K. Chu and L. G. Johnson, "Measurement of the development and evolution of shock waves in a laser-induced breakdown plasma," Phys. Fluids, 18, No. 11 (1975).
11. S. P. Popov, "Numerical calculation on the cooling of a spherical volume of nonequilibrium-ionized helium," Zh. Prikl. Mekh. Tekh. Fiz., No. 2 (1976).
12. Ya. B. Zel'dovich and Yu. P. Raizer, Physics of Shock Waves and High-Temperature Hydrodynamic Phenomena [in Russian], Nauka, Moscow (1966).
13. O. G. Firsov and M. I. Chibisov, "Emission from collisions of slow electrons with neutral atoms," Zh. Eksp. Teor. Fiz., 39, No. 6 (1960).